Flow Porometry:
What Can Flow Porometry Do For Us?

Akshaya Jena and Krishna Gupta.
Porous materials, Inc.
83 Brown Road, Ithaca, NY 14850, USA

Abstract

Use of modern technology has made flow porometry a very powerful and versatile tool for determination of a wide variety of pore structure characteristics of filtration media. The technique is described. Test results have been presented to demonstrate the use of the technique for measurement of pore structure characteristics. Measurable characteristics include the constricted pore diameter, the largest pore diameter, the mean flow pore diameter, pore distribution, gas permeability, liquid permeability, envelope surface area and effects of operational variables such as temperature, pressure, chemical environment and stress. Applications of the technique including pore characteristics in the thickness direction, pore characteristics in the x-y plane, properties of individual layers of multi-layered products determined in-situ without separating the layers and evaluation of properties without cutting samples and damaging the products, have been illustrated.

Introduction

Filtration media may contain three kinds of pores; closed pores, blind pores and through pores (Figure 1). Closed pores are not accessible. Blind pores do not permit flow. Through pores permit flow. The diameter of the through pore at its most constricted part determines flow and is equal to size of the smallest particle that would be prevented from passing through the filtration media (Figure 2a). The largest through pore constricted diameter, the mean flow pore diameter and the pore distribution determine the efficiency of separation by the filtration media. Similarly, Liquid permeability determines the rate of the filtration process. For separation of small solids from gases, external surface area (surface area of through pores) is important because small particles tend to stick to the surface (Figure 2b). The rates of such filtration processes are determined by gas permeability. All these important characteristics and the effects of operational variables can be determined by a single instrument based on flow porometry. No other instrument is capable of such versatility. The technique and its applications are discussed in this paper.

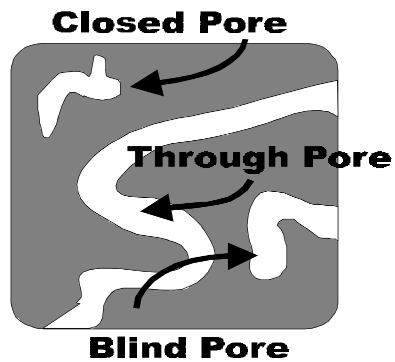

Figure 1. Three possible kinds of pores.

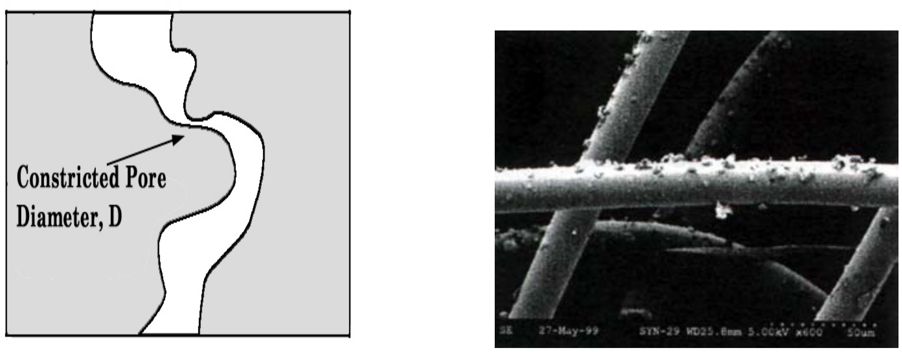

(a) Constricted pore diameter (b) Envelope (external) surface area

Figure 2. Important characteristics of porous media for filtration

Flow Porometry

Principle

A liquid is selected that does not react with the sample and spontaneously fills the pores of the sample (wetting liquid) [1]. A pressurized non-reacting gas is used to remove liquid from pores and permit gas flow (Figure 3).

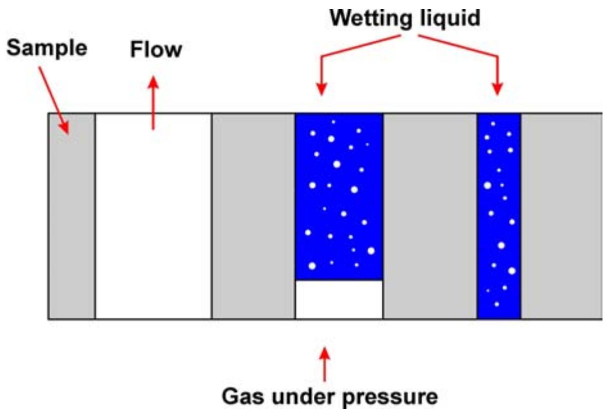

Figure 3. Principle of flow porometry.

The differential pressure needed to empty a pore is related to its diameter, D [2].

$$D = 4\gamma\cos\theta / p \qquad (1)$$

where γ is the surface tension of wetting liquid, θ is the contact angle and p is the differential pressure across the pore. It has been shown that for small surface tension liquids the contact angle may be assumed to be close to zero [1]. Equation 1 is used along with gas flow rates through wet and dry samples measured as functions of differential pressure to compute constricted pore diameters, the largest pore diameter, mean flow pore diameter, pore distribution, gas permeability and external surface area (Figure 4). Liquid permeability is computed from liquid flow rates through dry sample measured as a function of differential pressure.

(a)

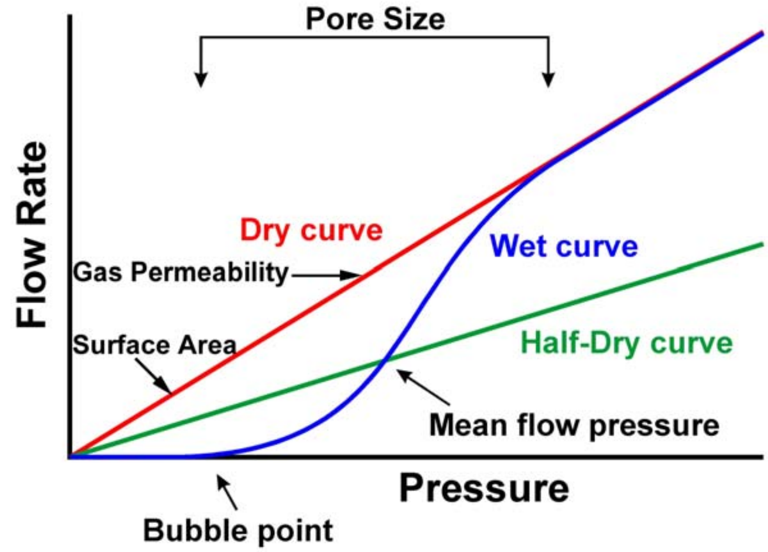

(b)

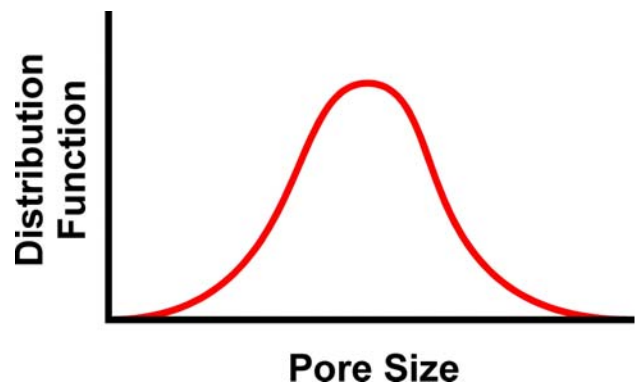

Figure 4. Pore characteristics obtainable from measured flow rates and pressures. Wet and dry curves represent flows through wet and dry samples respectively. Half-dry curve is computed to yield half of the flow rate through dry sample (dry curve). (a) Pore diameters and permeability. (b) pore distribution.

Definition of pore diameter

Equating the work done by the gas in displacing the liquid at a certain location in the pore to the increase in surface free energy due to replacement of liquid/solid surface by the gas/solid surface, it can be shown that [2]:

$$PdV = \gamma \cos \theta \, dS \quad (2)$$

where dV is the volume of liquid displaced in the pore and dS is the increase in the gas/solid interfacial area (decrease in the liquid/solid interfacial area). Pore diameter D is defined (Figure 5) such that:

$$[dS / dV]_{\text{pore}} = [dS / dV]_{\text{circular opening of diameter D}} = 4/D \quad (3)$$

Equation 1 follows from Equations 2 & 3.

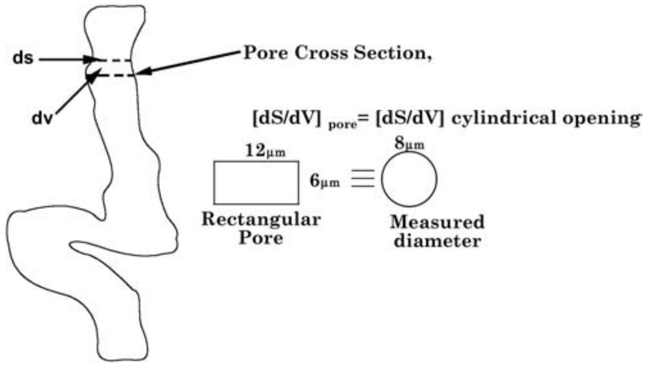

Figure 5. Definition of [pore diameter.

Constricted Pore Diameter

Pressure of gas required to displace the liquid in a pore increases with decrease in pore diameter. The pressure is maximum at the most constricted part of the pore. Once this maximum pressure is reached, liquid remaining in the rest of the pore and requiring less pressure is completely removed, gas flow starts through the pore and is sensed by the porometer and the presence of the pore is detected. Thus, the pressure for initiating flow through a pore is measured and therefore, the measured pressure gives the diameter of the pore at its most constricted part (Figure 6).

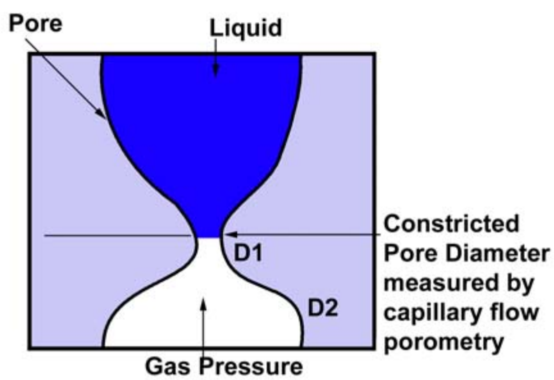

Figure 6. Constricted pore diameter measured by flow porometry.

Technology

In this investigation the PMI Capillary Flow Porometer was used (Figure 7). Test execution, data acquisition, data storage and data reduction were fully automated. The windows based operation was simple. State-of-the-art components and innovative design features resulted in highly reproducible results. The accuracy of results is demonstrated by the data in Table 1.

Figure 7. The PMI Capillary Flow Porometer.

Table 1 Comparison of pore diameters measured by the PMI Capillary Flow Porometer with those measured by SEM.
.

		Pore diameter, µm	
Sample	SEM Micrograph	SEM	PMI Porometer
Etched stainless steel disc	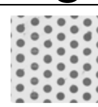	81.7 ± 5.2	86.7 ± 4.1
Polycarbonate membrane	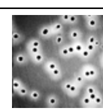	4.5 ± 0.5	4.6 ± 0.1

Applications

Pore structure in the z-direction (Thickness direction)

Typical data obtained using the flow porometer are shown in Figure 8. The data in this figure can yield many pore characteristics.

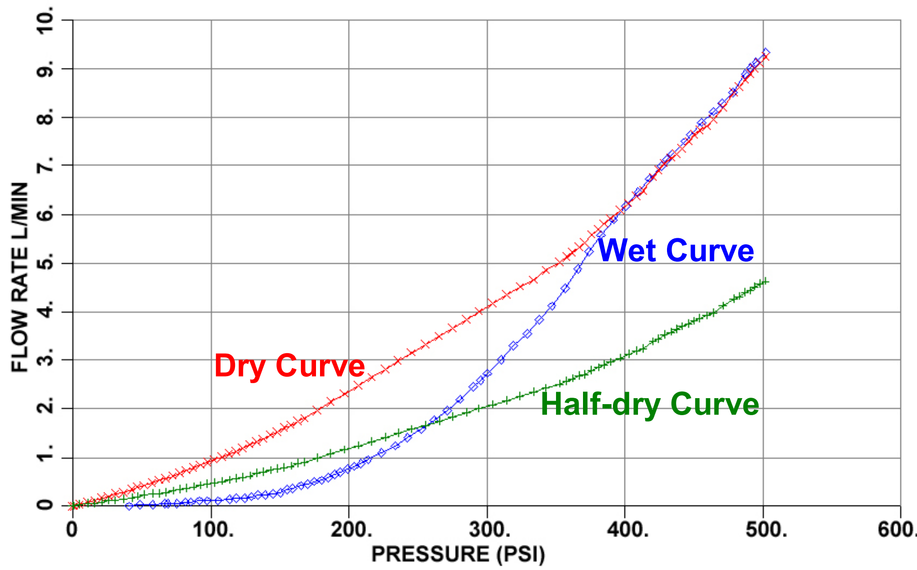

Figure 8. Flow rates measured as functions of differential pressure through a ceramic filter material.

The flow distribution derived from these data is presented in Figure 9 in terms of the distribution function, f.

$$f = - d[100\times(Fw/Fd)] / dD \quad (4)$$

where Fw and Fd are flow rates through wet and dry samples. The area under the curve in any pore diameter range gives percentage of flow through that range. It has been shown that the distribution curve is generally close to the pore number fraction in the filtration media [3]. The results of analysis of the measured data are tabulated in Table 2.

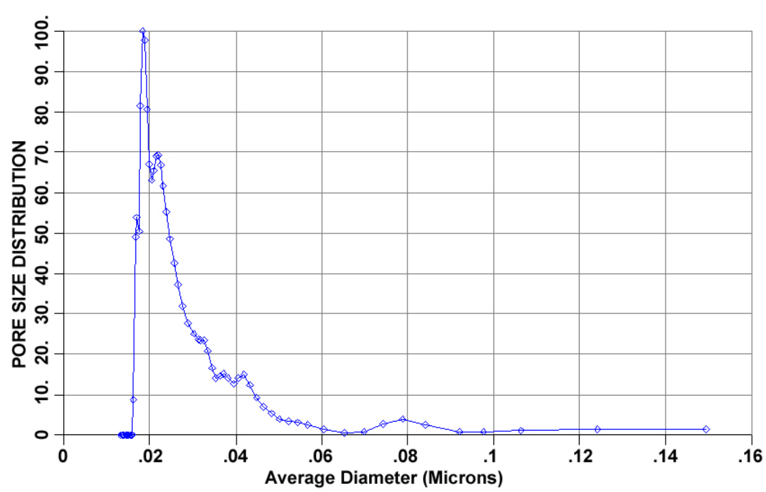

Figure 9. Flow distribution over pore diameter.

Table 2. Pore characteristics of filtration media obtained from data in Figure 8.

Characteristics	Values
The largest constricted pore diameter	0.1640 mµ
Mean flow constricted pore diameter	0.0256 mµ
Constricted pore diameter range	0.164 - 0.016 mµ
Peak of unimodal distribution	0.02 mµ
Constricted pore diameter range of most pores	0.164 - 0.064 mµ

Gas permeability

Gas permeability is obtained from the gas flow rates through a dry filtration medium measured as a function of differential pressure. Figure 10 shows data obtained with a ceramic filtration medium. The average air permeability calculated from the flow rates is 3.7×10^{-6} Darcies. The permeability can also be expressed in any other desired unit such as Frazier, Gurley, Rayls and volume /unit time-unit area-unit pressure gradient. One advantage of flow porometry is that permeability could be measured as a function of pressure.

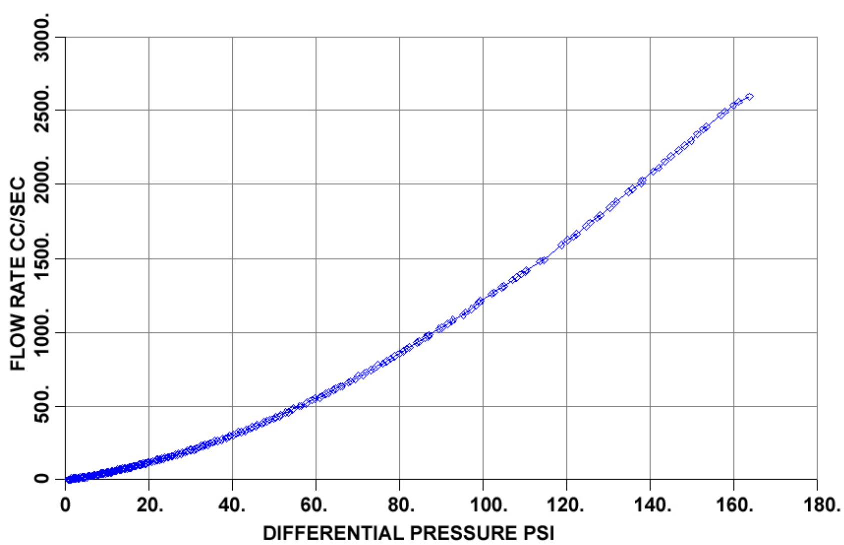

Figure 10. Air flow rate through a ceramic filtration medium.

Liquid permeability

Liquid permeability is obtained from the liquid flow rates through filtration media. Liquid flow rate of a strong chemical through a filtration medium is shown in Figure 11 as a function of pressure. The permeability can be expressed in any desired unit. The permeability can also be computed as a function of pressure.

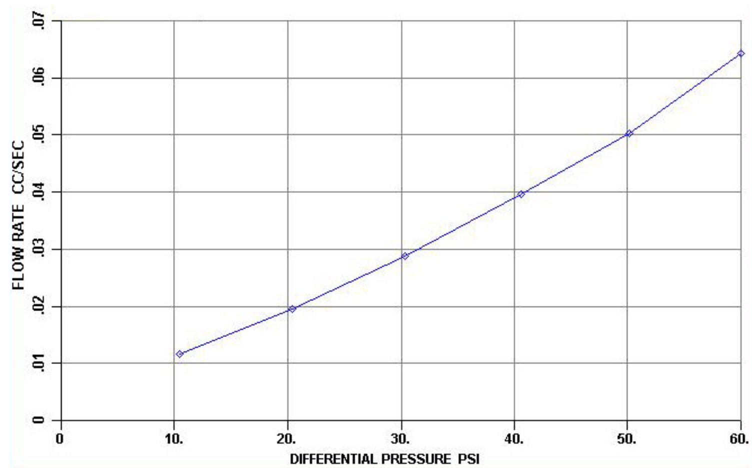

Figure 11. Liquid flow rate of 31% KOH solution through a nonwoven.

Envelope surface area

The envelope surface area is the surface area of through pores (Figure 1) that permit gas flow. Using flow rate and differential pressure data the envelope surface area is calculated with the help of Kozeny-Carman relation [4]. Figure 12 shows surface area as a function of flow rate through a filtration medium. As expected the surface area is insensitive to flow rate. The surface area measured by this technique compares very well with the surface area measured by gas adsorption technique for materials with negligible blind pores (Figure 1).

Battery separator Surface Area: Porometter 0.56 m^2/g
BET 0.52 m^2/g

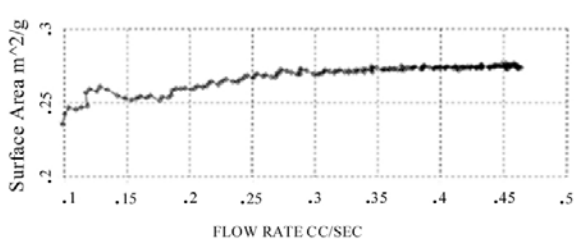

Figure 12. Surface area of a fibrous mat measured as a function of flow rate.

Average fiber diameter

The average fiber diameter is computed from the flow rate using the Davies [5] equation. The measured average fiber diameters compare very well the directly measured average fiber diameters. This is demonstrated by the data in Figure 13.

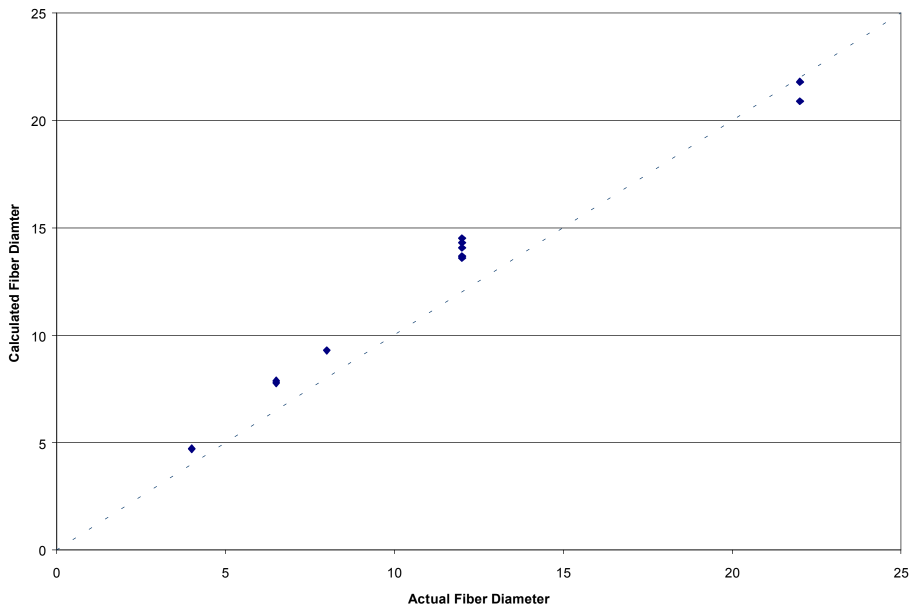

Figure13. Measured average fiber diameters plotted against the actual fiber diameters in a nonwoven filtration medium.

Effects of orientation (Pore structure in the x-y plane)

Pore structure in the z-direction (thickness direction) can be considerably different from that in the x-y plane of a material (Figure 14). These pore characteristics can be measured by the capillary flow porometer.

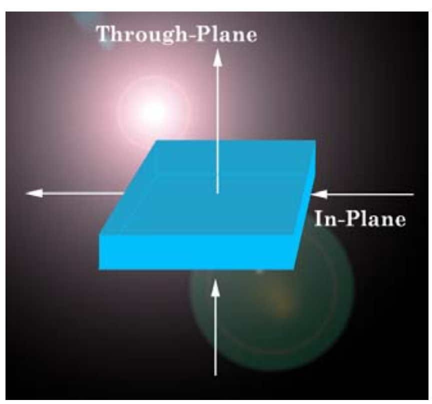

Figure 14. Directional pore structure.

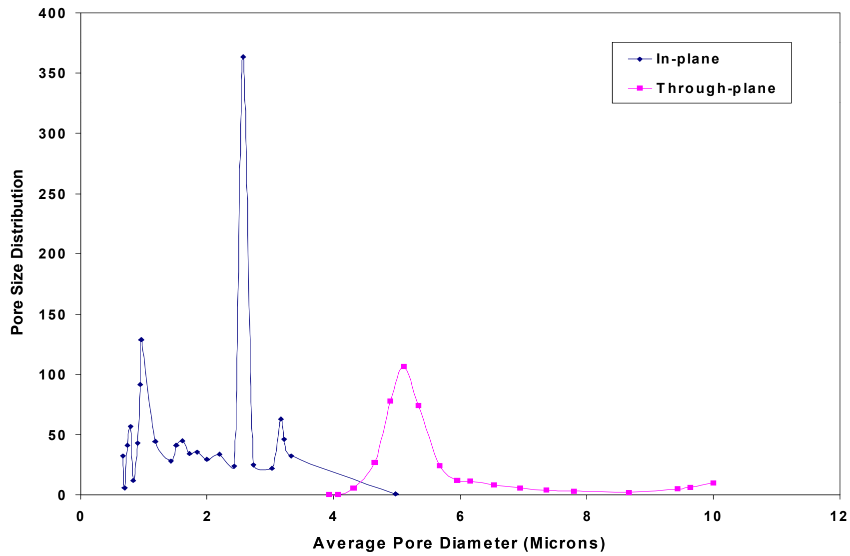

Figure 15. Widely different pore distributions along the thickness (z-direction) and in the the x-y plane of a nonwoven filter material.

Effects of temperature

The instrument can measure pore characteristics at temperatures up to 100° C. Gas and liquid permeability can be measured up to 200° C. Figure 16 shows data on gas permeability measured at two temperatures.

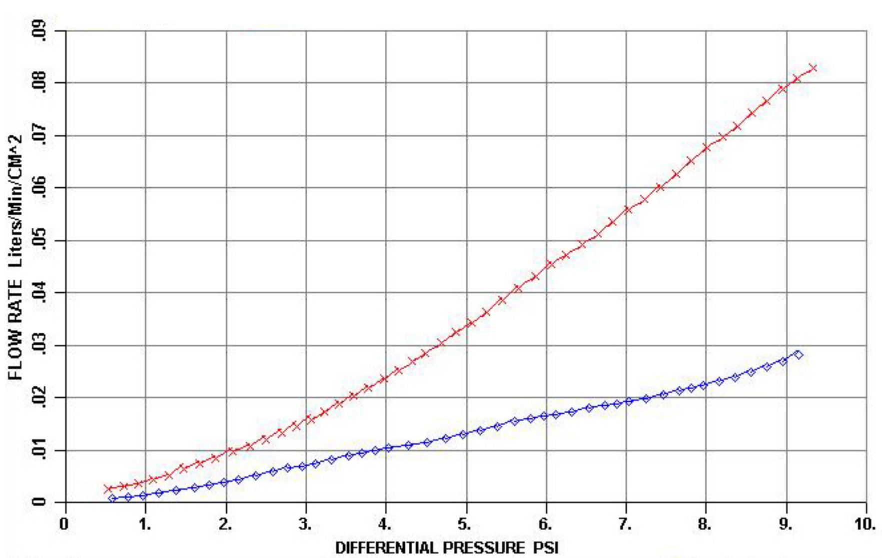

Figure 16. Air permeability at 70 °C and 20 °C.

Effects of chemical environment

Tests can be performed with liquids of interest. Sample saturated in desired chemical can be tested. Chemicals used in applications can be used as wetting liquids. Strong chemicals like phosphoric acid, KOH and saline solutions can be used for the test. Figure 17 shows the results of a pore structure characterization performed using a KOH solution.

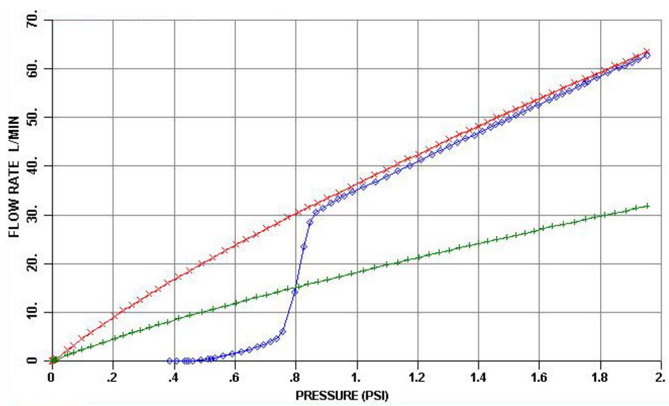

Figure 17. Pore structure characteristics of a separator determined using KOH solution.

Effect of pressure

Liquid permeability at pressures up to 200 psi can be measured. The data in Figure 18 gives permeability up to 160 psi.

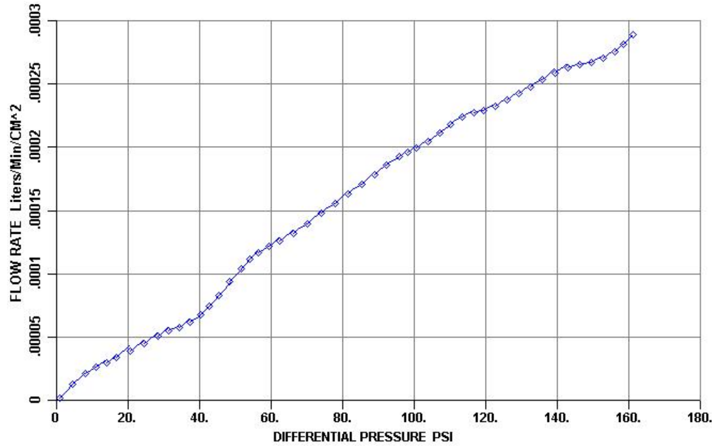

Figure 18 Permeability at 160 PSI

Effects of compressive stress

During application, most filtration media are subjected to stress. Stress can change pore structure appreciably. Filter media maintained under compressive stress could be tested for changes in their pore characteristics. Figure 19 shows that the effects of stress can be considerable.

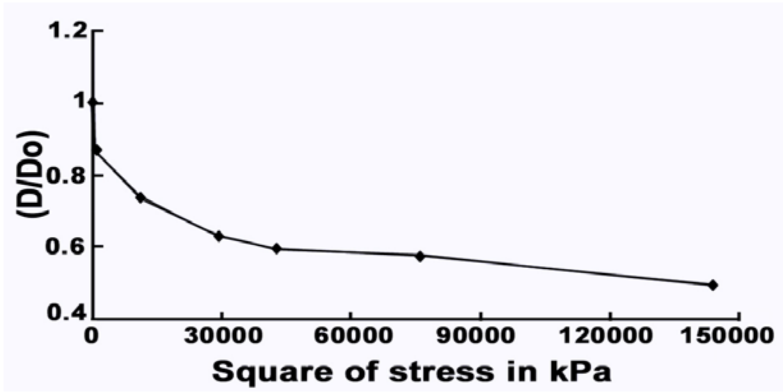

Figure 19. Effect of compressive stress up to 1200 kPa on bubble point pore diameter.

Effects of stress cycles

In many applications like dewatering of paper pulp, the filtration media are subjected to cyclic stress. Stress cycles may change pore characteristics considerably. Figure 20 shows the effects of cyclic stress on a nonwoven material.

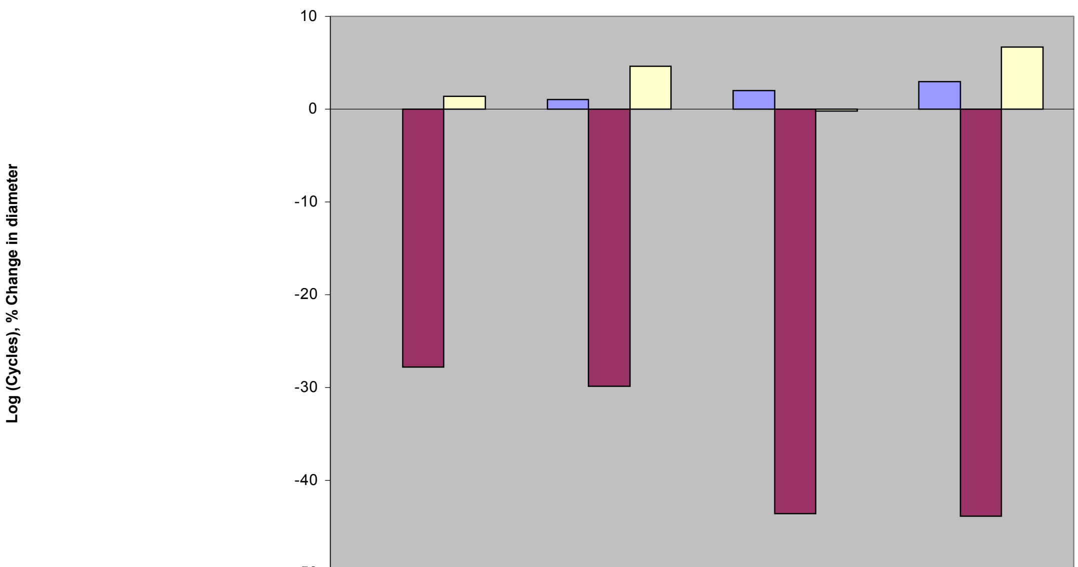

	1	2	3	4
Log (Cycles)	0	1	2	3
% Change in bubble point pore diameter	-27.8	-29.9	-43.6	-43.9
% Change in mean flow pore diameter	1.4	4.6	-0.2	6.7

Figure 20. Effects of number of stress cycles between 15 and 35 psi on % changes in the bubble point pore diameter and mean flow pore diameter

Pore structures of individual layers of a two-layer filtration media without separating the layers.

The instrument can measure pore structure characteristics of individual layers of a multi layered filtration media without separating the layers. The instrument can also measure graded pore structure. The principle of the test technique is illustrated in Figure

21 [6]. The considerably different pore sizes in the two separate layers of a hot gas ceramic filter is shown in Figure 22.

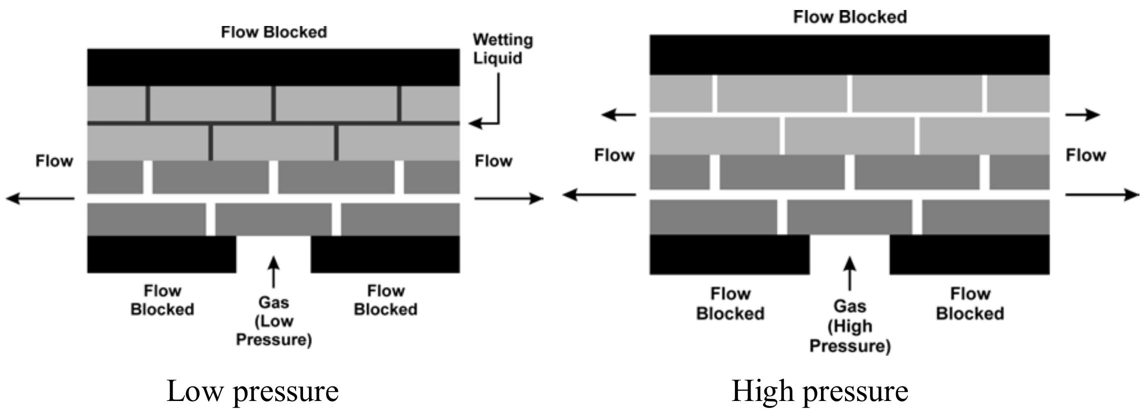

Figure 21. Techniques for determination of pore structure of layered or graded filtration media.

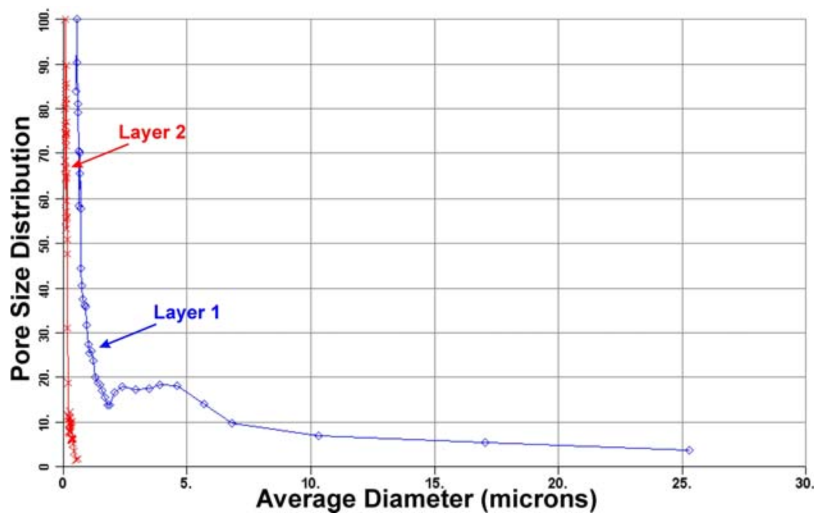

Figure 22. Considerably different pores of the two layers of a ceramic hot gas filtration media determined in-situ without separating the layers.

On-line characterization of pore structure

The instrument chamber of the on-line capillary flow porometer is so designed that samples are not required to be cut from a bulk material. The test head either clamps on to the area to be tested on any part of the final product or the product may be made to slide through the test head. This design of the instrument permits tests to be performed on any part of huge rolls of products for evaluation of homogeneity, suitability of materials for applications and process control without damaging the material in any way. Two test head systems are shown in Figure 23.

(b) Slide through.

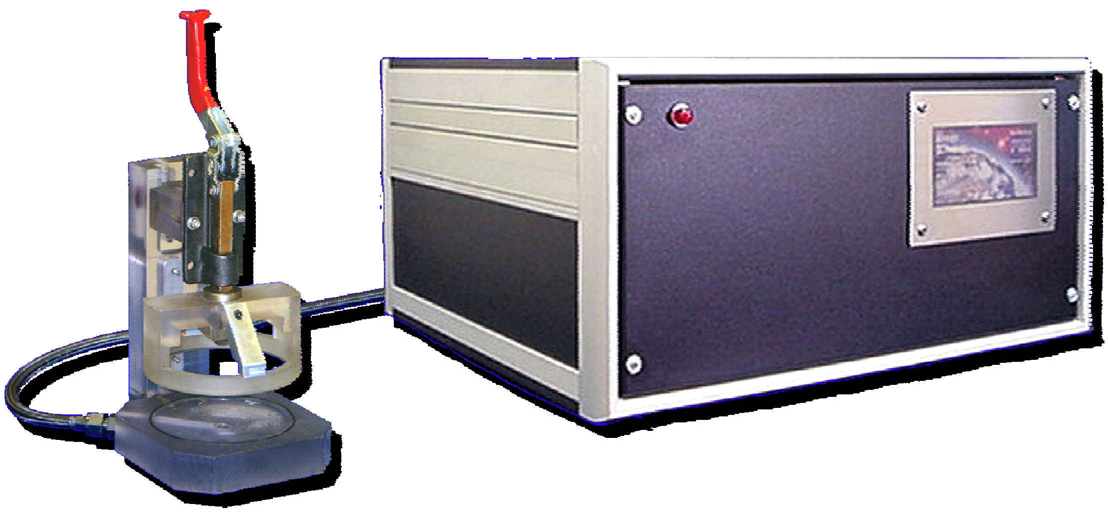

(a) Clamp on.

Figure 23. Two test heads of the PMI On-Line Porometer

Summary and Conclusion

1. Principle of flow porometry, its potentials and its limitations have been discussed.
2. Many applications of the technique have been demonstrated using the PMI Capillary Flow Porometer.
3. Constricted pore diameters, the largest pore diameter, mean flow pore diameter, pore distribution, envelope surface area, average fiber diameter, gas permeability and liquid permeability were measured. The effects of temperature, pressure, chemical environment, compressive stress, stress cycles, and orientation were also measured. Determination of pore structures of individual layers of multi-layered structures, pore structures in thickness direction as well as in the x-y plane and pore structures at

many locations of large filtration media without damaging the material in any way were demonstrated.

4. Capillary flow porometer is a highly versatile instrument capable of measuring all the important pore structure characteristics of filtration media.

References

1. Vibhor Gupta and A. K. Jena, Advances in Filtration and Separation Technology, American Filtration & Separation Society, 13b (1999), 833.
2. A. K. Jena and K. M. Gupta, Journal of Power Sources, 80 (1999), 46.
3. A. K. Jena and K.M. Gupta, Proceedings of International Conference Filtration 99, Chicago, INDA (Association of the Nonwoven Fabrics Industry), Book of Papers, 23.1.
4. Gerard Kraus, J.W. Ross and L A. Girifalco, Phys. Chem., Vol. 57. 1953, pp. 330-333.
5. C.N. Davies, Proceedings of the Institute of Mechanical Engineers, London, 1B, 1952, pp.185-194.
6. A. Jena and K. Gupta, F &S Filtrieren und Separieren, 16 (2002), 13.